Electronic Supplementary Material (ESI) for Nanoscale.

Electronic Supplementary Information Charge Transport in MBE-grown $2H - MoTe_2$ Bilayers with Enhanced Stability Provided by AlO_x Capping Layer.

Zuzanna Ogorzałek[a], Bartłomiej Seredyński[a], Sławomir Kret[b], Adam Kwiatkowski[a], Krzysztof P. Korona[a], Magdalena Grzeszczyk[a], Janusz Mierzejewski[a], Dariusz Wasik[a], Wojciech Pacuski[a], Janusz Sadowski[a],[b,‡], and Marta Gryglas-Borysiewicz[a*]

E-mail: marta.borysiewicz@fuw.edu.pl

[a]*Faculty of Physics, University of Warsaw, Pasteura 5, 02-093, Warsaw, Poland*
[b]*Institute of Physics, Polish Academy of Sciences, al. Lotnikow 32/46, 02-668, Warsaw, Poland*
‡*Department of Physics and Electrical Engineering, Linnaeus University, SE-391 82 Kalmar, Sweden*
**Corresponding author*

In the following paragraphs we apply different models of electron transport to our transport data. The general form of the conductivity (T) dependence is given by: $\sigma(T) = \sigma_0 \cdot exp[-(T_0/T)^x]$, where x changes for various transport mechanisms. For the variable hopping rage model where the density of states is gapless and there is no electron-electron interactions the conductivity dependence changes with the temperature as $T^{-1/4}$ for 3-dimentional systems and as $T^{-1/3}$ for 2-dimentional systems. If the electron-electron interactions take place, the variable range hopping occurs with $x = \frac{1}{2}$. Figures S1(a)-(b) show the relation between conductivity and temperature for the capped sample for various transport mechanisms. The green and orange curves present the Mott-Davis variable range hopping models. The grey and black curves show the conductivity dependece for Efros-Shklovskii variable range hopping and the band transport models, respectively. Blue curve corresponds to anomalous exponent of $x \simeq 0.66$.

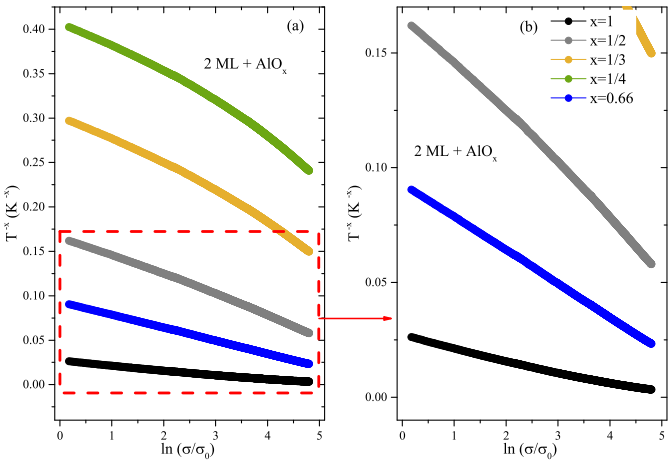

Figure S1: Various conductivity models for the capped sample.

In further sections **1** and **2** we present the detailed studies of the choosen models.

1 Band transport (hopping exponent = 1)

Although band transport model does not fit the whole temperature range, it can be applied to some parts of data. Figure S2 presents the resistivity of the uncapped and capped samples as a function of the inverse temperature. A fit of ρ=$\rho_0 \cdot \exp(E_a/k_B T)$, where $\rho_0 = 1\ \Omega \cdot cm$ provides activation energies E_a below T=100 K: $\approx 14\ meV$ and $\approx 13\ meV$ for the uncapped and capped $MoTe_2$, respectively. Above T=150 K: $\approx 27\ meV$ and $\approx 21\ meV$ for uncapped and capped 2 ML, respectively.

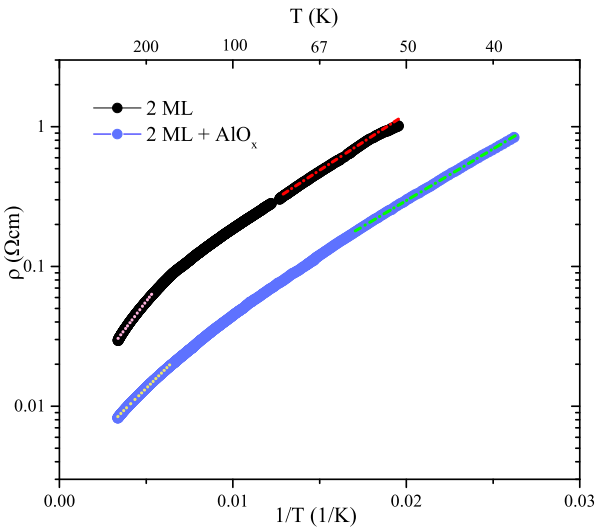

Figure S2: The resistivity as a funcion of inverse temperature for the uncapped and capped samples. Dashed lines show fitted curves.

They are considerably smaller than energy gap of $2H - MoTe_2$ (E_g ≈1 eV) and reasonably correspond to the energies of shallow impurities in $2H - MoTe_2$. The obtained values of activation energies are similar to energies observed before, for thicker TMD layers, grown by molecular beam epitaxy.[1,2]

2 Hopping transport (hopping exponent = $\frac{1}{2}$ or $\frac{1}{4}$)

Variable range hopping model was applied to analyse the data. The conductivity is given

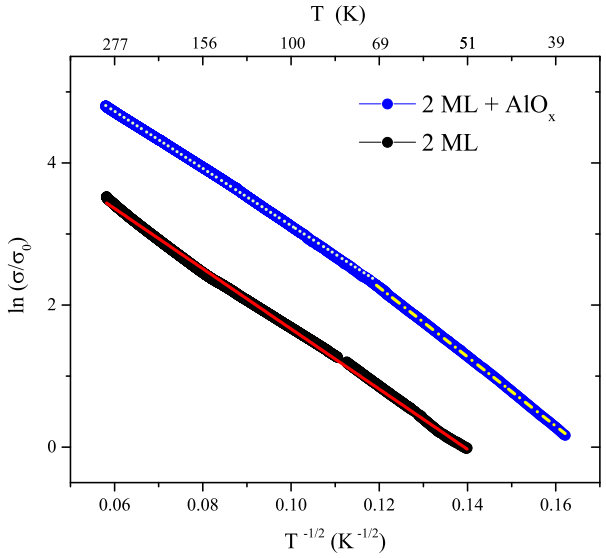

Figure S3: The conductivity as a function of inverse temperature for the uncapped and capped samples with Efros-Shklovskii model. Dashed lines show fitted curves.

by the $\sigma(T) = \sigma_0 exp(-(\frac{T_0}{T})^{\frac{1}{2}})$ expression, where T_0 and σ_0 are constant parameters. The two parameters carry important information about the hopping process: the optimal hopping distance (d_h) and energy difference (E_h). They are given by $d_h = 0.25 \cdot \alpha^{-1}(\frac{T_0}{T})^{\frac{1}{2}}$ and $E_h = 0.5 \cdot k_B (T_0 T)^{\frac{1}{2}}$,[3] where $\alpha = \frac{T_0 4\pi\varepsilon_0\varepsilon_r k_B}{\beta e^2}$, β - parameter of the order of unity,[4] e - elementary charge, ε_0 - absolute permittivity, ε_r - relative permittivity ($\varepsilon_{r\perp}$=9.6 and $\varepsilon_{r\parallel}$=21.6 - anisotropic for bilayer of $2H - MoTe_2$).[5] Figure S3 presents the conductivity of the capped and uncapped samples as a function of $T^{-\frac{1}{2}}$ with fits. The value of T_0 is presented in Table S1. Figures S4(a)-(b) show the calculated values of the optimal hopping distances and energies as a function of temperature, for an average value of relative permittivity, respectively. The optimal hopping distance stays very low for both samples, and equals about 1 nm. The hopping energy is of the order of few tens of meV. The similar values of optimal hopping distances and hopping energies show that despite the capping layer, the charge transport is similar for both samples.

Figure S5 presents the conductivity of the capped sample as a function of temperature

Table S1: T_0 parameters obtained from Efros-Shklovskii variable-range hopping model.

Sample:	2 ML	2 ML + AlO_x
T_0 [K]	1776 ± 88	2409 ± 58 ($T < 67$ K) 1659 ± 66 ($T > 67$ K)

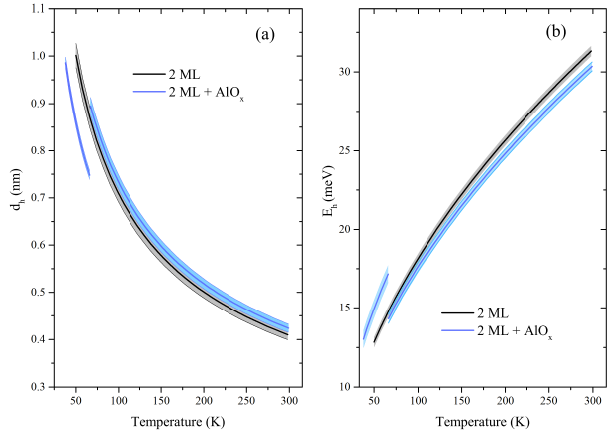

Figure S4: The dependence of (a) the optimal hopping distances on the temperature and (b) optimal hopping energies on the temperature for the uncapped and capped samples for $< \varepsilon_r >$=14.4. The double dependence for the capped sample results from a change in the curve slope in its conductivity (see Figure S3 at $T \simeq 67$ K) and bilinear fit. The strips around the calculated curves present the standard deviation of the mean.

with the value of the hopping exponent $x = \frac{1}{4}$ (see green curve in the Figure S1) with fitted lines at the periferies of $\rho(T)$ curves. Although one can fit linear dependences locally, the overall character of $\rho(T)$ dependence does not agree with nearest-neighbour hopping model.

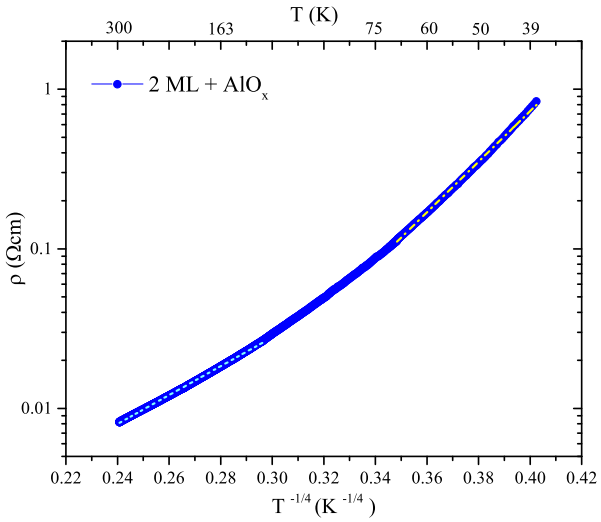

Figure S5: The conductivity as a function of inverse temperature for capped sample with Mott-Davis model. Dashed lines show fitted curves.

References

(1) Roy, A.; Movva, H. C. P.; Satpati, B.; Kim, K.; Dey, R.; Rai, A.; Pramanik, T.; Guchhait, S.; Tutuc, E.; Banerjee, S. K. Structural and Electrical Properties of $MoTe_2$ and $MoSe_2$ Grown by Molecular Beam Epitaxy. *ACS Appl. Mater. Interfaces* **2016**, *8*, 7396–7402.

(2) He, Q.; Li, P.; Wu, Z.; Yuan, B.; Luo, Z.; Yang, W.; Liu, J.; Cao, G.; Zhang, W.; Shen, Y.; Zhang, P.; Liu, S.; Shao, G.; Yao, Z. Molecular Beam Epitaxy Scalable Growth of Wafer-Scale Continuous Semiconducting Monolayer $MoTe_2$ on Inert Amorphous Dielectrics. *Adv. Mater.* **2019**, *31*, 1901578.

(3) Shklovskii, B.; Efros, A. In *Electronic Properties of Doped Semiconductors*; Luryi, S., Ed.; Springer-Verlag Berlin Heidelberg: Tiergartenstrasse 17, D-69121 Heidelberg, Germany, 1984; p 388.

(4) Adkins, C. J. Conduction in granular metals-variable-range hopping in a Coulomb gap? *J. Phys. Condens. Matter* **1989**, *1*, 1253–1259.

(5) Laturia, A.; Van de Put, M. L.; Vandenberghe, W. G. Dielectric properties of hexagonal boron nitride and transition metal dichalcogenides: from monolayer to bulk. *NPJ 2D Mater. Appl.* **2018**, *2*, 2397–7132.